



Salicylaldiminato chromium complex supported on chemically modified silica as highly active catalysts for the oxidation of cyclohexene

Salam J.J. Titinchi and Hanna S. Abbo

Abstract

Immobilization of chromium complexes on modified silica support was achieved via two different synthetic routes using 3-aminopropyl triethoxysilane (APTS) as a linking group. The FTIR spectra, elemental and solid-state NMR analyses demonstrated incorporation of amine functional groups on the surface of the APTS-functionalized silica support, which was further confirmed by ^{29}Si solid-state CP MAS NMR spectroscopy.

Oxidation of cyclohexene was carried out over the chromium complex supported on organically modified silica using H_2O_2 as an oxidant under various conditions and different atmospheres viz. oxygen, nitrogen and air. The supported catalysts exhibited excellent activity (>94%) after 6 h reaction time under O_2 atmosphere using THF as solvent. The catalysts showed high chemoselectivity towards formation 2-cyclohexen-1-ol and 2-cyclohexen-1-one. Activity of the immobilized catalysts remains nearly the same after three consecutive cycles, suggesting the true heterogeneous nature of the catalyst.

1. Introduction

In recent years, heterogenization of organocatalytic systems has been achieved by immobilization of homogeneous catalysts on various types of organic and inorganic supports. These heterogeneous systems have received serious attention as alternatives to conventional homogeneous catalysts. Several immobilization strategies have been widely applied for creating active sites on the support surface [1–3]. Surface modification using organic functional groups has been found to be useful for their immobilization on the silica surface, which represents a significant feature of the catalyst heterogenization [4]. Use of inorganic supports with chemically bound active centres as heterogenized catalysts provides the homogeneous systems with attractive features and additional advantages such as catalyst stability, easy separation, handling, and recovery to reduce environmental problems [5].

3-Aminopropyltrialkoxysilane is one of the most commonly used precursors for the modification of silica surfaces [6,7]. Furthermore, amino-functionalized silica plays a vital role in the development of materials for several applications, such as adsorption of metal ions [8], enzyme immobilization [9], drug delivery [10] and catalysis [11].

Functionalization of mesoporous silica surfaces by the immobilization of active sites via tethering or grafting methods have been developed to covalently attach transition-metal complexes to mesoporous inorganic materials. These methods overcome the problems of metal leaching in comparison with the ion exchange or adsorption methods used for immobilization on porous supports. The silica mesoporous material with pore size $>20 \text{ \AA}$ is well-known to be suitable for liquid-phase reactions that allow easy diffusion of reactants to the active sites [4]. Thus, the silica material utilized in this work with pore size of 88 \AA was used as a support for chromium complexes in liquid phase oxidation of cyclohexene.

Catalytic oxidation of cyclohexene by peroxides is of both chemical and biochemical interest due to the formation of different oxygenated functionalized products. These products are very important as starting materials in pharmaceutical industries and in synthesizing fine chemicals [12].

There are several reports on homogenous chromium–salen complexes as catalysts for alkene oxidation [13]. Also a variety of chromium-based reagents have been used as catalysts for selective oxidation of allylic compounds [14]. Recently, Kawanami et al. [15], Shiraishi et al. [16] and Mohapatra et al. [17] described their studies on the oxidation of olefins with molecular O_2 using Cr-containing mesoporous molecular sieves in which Cr metal was directly incorporated within the silica matrix. Jacobs and Dooos have prepared dimeric Cr(III)salen impregnated or supported on silica for epoxide ring opening reactions [18].

To date, several reports on chromium complexes immobilized on functionalized silica have been reported for various oxidation reactions particularly epoxidation [19,20] and epoxide ring opening reaction [21]. On the other hand, Koner et al. described Cu(II) complex supported catalysts containing a ligand derived from salicylaldehyde and APTS anchored on MCM-41 [22]. The resulting catalyst was shown to be highly efficient for epoxidation of olefins using *tert*-BuOOH (TBHP) as an oxidant.

Catalysts employed in this paper are based on the salicylaldehyde chromium(III) complex bound to a silica gel surface via the hydrophobic propylsilane linking group between organic moieties and inorganic support. The modified silica gel supported chromium(III) catalysts were synthesized via two synthetic routes, characterized and screened for the liquid phase catalytic oxidation of cyclohexene with hydrogen peroxide.

2. Experimental

2.1 Materials

Salicylaldehyde, (3-aminopropyl)triethoxysilane, silica gel (Davisil, grade 710, 4–20 μ , 60°, 99%), chromium acetate hydroxide [$\text{Cr}_3(\text{CH}_3\text{COO})_7(\text{OH})_2$], chromium trichloride anhydrous, 30% aqueous H_2O_2 , cyclohexene redistilled), cyclohexene oxide, 2-cyclohexen-1-ol, 2-cyclohexen-1-one, 1,2-cyclohexandiol were purchased from Aldrich, tetrahydrofuran from Sarachem, acetonitrile from Riedel-de Haen. 1,2-Dichloroethane, benzene, ethanol and acetone from Sigma-Aldrich.

2.2 Physical methods and analysis

^1H and ^{13}C NMR spectra were recorded in CDCl_3 using a Varian XR200 spectrometer (^1H at 200 MHz, ^{13}C at 50.3 MHz). Sample signals are relative to the resonance of residual protons on carbons in the solvent. The solid-state NMR was carried out on a Varian VNMRs 500 MHz two channel spectrometer using 6 mm zirconia rotors and a 6 mm Chemagnetics TM T3 HX probe. The direct polarization (DP/SPE) spectrum was recorded at ambient temperature with proton decoupling, a 3.75 μs 90° pulse, and a recycle delay of 30 s. All cross-polarization (CP) spectra were recorded at ambient temperature with proton decoupling, a 3.75 μs 90° pulse, and a recycle delay of 5 s. The power parameters were optimised for the Hartmann-Hahn match. The contact times for cross-polarization was 1 ms. The free induction decay for both was 640 points, Fourier transformed with 1280 points and 50 Hz line broadening. Magic-angle-spinning (MAS) was performed at 5 kHz and adamantane was used as an external chemical shift standard.

The elemental analysis was performed on a Carlo Erba analyzer, thermal analysis using Mettler Toledo TGA/SDTA and the BET surface area using a Tristar 3000 micromeritics Surface Area and Porosity Analyzer at the University of Cape Town, South Africa. The percentage metal content was determined using Pye Unicam 9100 atomic absorption spectrophotometer and ICP. The ATR-IR measurements were carried out on a Perkin-Elmer Spectrum 100 FTIR spectrometer and Paragon 1000 PC FT-IR spectrometer. Electronic spectra were recorded on a GBC UV/VIS 920 UV-Visible spectrophotometer in absolute ethanol or in Nujol (by layering the mull of the sample to the inside of one of the cuvette while keeping another one layered with Nujol as reference). In some cases a diffuse reflectance technique was used (recorded under ambient conditions equipped with a quartz cell). All catalyzed reaction products were analyzed using Varian CP3800 gas chromatograph fitted with flame ionization detector. A HP-PONA capillary column (50 m \times 0.35 mm (id) \times 0.5 μm film thickness, Agilent technologies, J&W Scientific) and Star workstation computer software were used. The retention time of all the peaks were compared with authentic samples and from GC-MS data.

2.3. Preparations

All reactions were performed under a dry nitrogen atmosphere using standard Schlenk techniques. Freshly dried ethanol (dried by standard method; distillation over magnesium turnings and iodine). Solvent was degassed with nitrogen for 15 min prior to the catalytic tests.

2.3.1 Synthesis and immobilization of the ligands and their Cr-complex

Preparation of Cr(III) salicylidene propylene silane supported on silica gel.

Two different synthetic routes were followed to prepare this catalyst (Scheme 1).

2.3.1.1 Route 1 (Pre-grafting): Ligand – Complexation – Immobilization (L.C.I.).

2.3.1.2 Preparation of 2[(E)-{(3-triethoxysilyl)propyl}imino]phenol

(APTSSal) (L1). Equal moles of (3-aminopropyl)-triethoxysilane (APTS) (2.77 g, 12.5 mmol) and salicylaldehyde (Sal) (1.53 g, 12.5 mmole) were dissolved in freshly dried ethanol (50 mL) under nitrogen atmosphere at room temperature. The reaction mixture immediately changed to yellow and was left to reflux for 3 h. A yellow semi-viscous liquid was obtained after evaporation of ethanol using a rotary evaporator (yield 3.59 g, 88%) which was characterized directly.

IR, $\nu = 1632 \text{ cm}^{-1}$ (C N); ^1H NMR (CDCl_3 , ppm): 13.56 (s, 1H, phenolic OH), 8.34 (s, 1H, CH N), 7.34–6.82 (m, 2H, phenyl 2-H and 3-H), 6.97–6.82 (m, 2H, phenyl 4-H and 5-H), 3.88–3.77 (q, 6H, CH_2O), 3.63–3.56 (t, 2H, CH_2N), 1.87–1.75 (quintet, 2H, 1,3-propyl CH_2), 1.26–1.19 (t, 9H, CH_3 of ethoxy group), 0.73–0.64 (t, 2H, CH_2Si); ^{13}C NMR (CDCl_3 , ppm): 7.63, 17.97, 24.09, 58.03, 61.60, 116.62, 118.00, 118.50, 130.84, 131.67, 161.12, 164.52. Anal. Calcd. for $\text{C}_{16}\text{H}_{27}\text{NO}_4\text{Si}$: C 59.1, H 8.31, N 4.31. Found: C 57.84, H 8.03, N 4.51.

2.3.1.1.2. Complexation (C1): $[\text{L}_4\text{Cr}_2(\mu\text{-OH})(\mu\text{-O}_2\text{CCH}_3)]$. Two different chromium metal sources were used to prepare the unsupported catalyst:

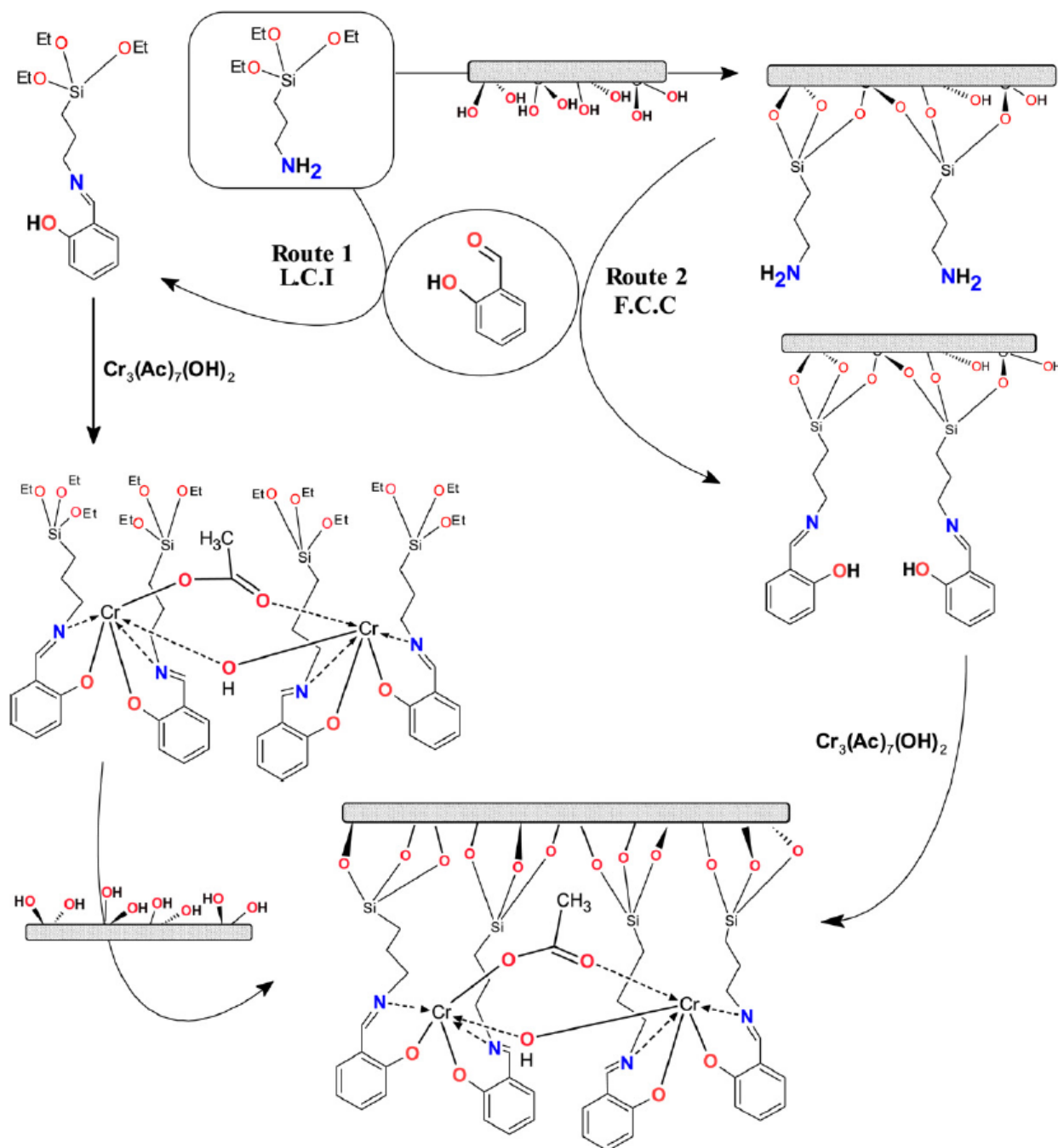
(i) Chromium acetate hydroxide: $\text{Cr}_3(\text{Ac})_7(\text{OH})_2$ (1.04 g, 1.7 mmol) was dissolved in dry ethanol (20 mL) and added to **L1** in 1:6 (Cr-acetate: APTSSal) molar ratio. The reaction mixture was refluxed with stirring overnight. A green semi-solid was obtained (5.4 g; yield 60%). IR, $\nu = 1614 \text{ cm}^{-1}$ (C N); 1712 cm^{-1} (C O). Anal. Calcd. for $\text{C}_{66}\text{H}_{108}\text{N}_4\text{O}_{19}\text{Si}_4\text{Cr}_2$: C 53.66, H 7.32, N 3.79. Found: C 51.93, H 7.32, N 3.79. Anal. by ICP (Atomic %): Cr, 6.91. M/N = 1.82; C/N = 13.70 (Calcd. 14.14).

(ii) Chromium chloride anhydrous: On the other hand using CrCl_3 anhydrous as a metal source, no complexation took place.

2.3.1.1.3. Immobilization. Silica gel (Davisil, grade 710, 4–20 μ) (5 g) was added directly to **C1** in dry ethanol (50 mL). The mixture was left to stir overnight under nitrogen atmosphere. A green solid (6.93 g) was obtained. The solid was filtered and washed thoroughly several times with boiling ethanol to get rid of any free metal salt immobilized on the silica surface. The resulting solid was oven dried at 80 °C for 3 h. IR, ν = 1614 cm^{-1} (C N); 1712 cm^{-1} (C O). Anal. Found: C, 4.03; N, 0.29; Anal. atomic % (ICP): Cr, 0.52. % M/N = 1.79; C/N = 13.90 (Calcd. 14.14).

2.3.1.3 Route 2 (post-grafting): Functionalization – Condensation – Complexation (F.C.C.).

2.3.1.3.1 Functionalization (SG-APTS). The inorganic support materials, was functionalized with amino groups. (3-Aminopropyl)-triethylsilane (2.77 g, 12.5 mmol) in dry ethanol (10 mL) was added directly to a suspension of silica gel (5.0 g) in



Scheme 1. Synthetic routes of Cr-supported catalyst.

dry ethanol (50 mL). The mixture was left to stir overnight under nitrogen atmosphere. A colourless solid was obtained, filtered and washed thoroughly several times with boiling dry ethanol to get rid of any unimmobilized silane. The resulting solid was oven dried at 80 °C for 3 h. (7.2 g), IR, $\nu = 1550 \text{ cm}^{-1}$ (symmetric NH₂ bending vibration). Anal. Found: C, 4.21; N, 1.64; C/N = 2.57 (Calcd. 2.57).

2.3.1.3.2 Preparation of supported salicylidene propylene triethoxy silane (SGPTSSal) (L2). An excess amount of salicylaldehyde (Sal) (1.53 g, 12.5 mmol) in dry ethanol (10 mL) was added to an equivalent mole of the assumed

moles of (3-aminopropyl)triethoxysilane attached to silica gel surface (APTS-SG) (2.7 g) in freshly dried ethanol (50 mL) in a Schlenk tube under nitrogen atmosphere. The reaction mixture immediately changed to yellow and was left to reflux for 3 h. A pale yellow powder was obtained (3.2 g). Anal. Found: C, 5.86; N, 0.44; IR, $\nu = 1632 \text{ cm}^{-1}$ (C N).

2.3.1.3.3 Complexation (C2). Chromium acetate hydroxide (1.04 g, 1.7 mmol) was dissolved in dry ethanol (20 mL) and added to the supported ligand (**L2**) suspended in ethanol (20 mL) in 1:6 (Cr-acetate:APTSal) molar ratio. The reaction mixture was refluxed with stirring overnight. A pale green powder was obtained (3.8 g). IR, $\nu = 1614 \text{ cm}^{-1}$ (C N); 1712 cm^{-1} (C O). Anal. Found: C, 4.32; N, 0.31; Anal. atomic % (ICP): Cr, 0.57. % M/N = 1.84; C/N = 13.94 (Calcd. 14.14).

2.4. Catalytic evaluation

Oxidation of cyclohexene using the prepared catalysts was carried out in a 12 place parallel reactor using 50 mL glass reactor vessels (a Radley's Discovery Technologies 12 place Heated Carousel Reaction Station fitted with a reflux unit as well as a gas distribution system). In a typical reaction, cyclohexene (2.05 g, 0.025 mol) and 30% solution of H_2O_2 (3.58 g, 0.025 mol) were mixed in 5 mL of the desired solvent unless otherwise stated, and the reaction mixture was heated at $80 \text{ }^\circ\text{C}$ with continuous stirring. Toluene was added as an internal standard. The reactions were carried out under an oxygen atmosphere.

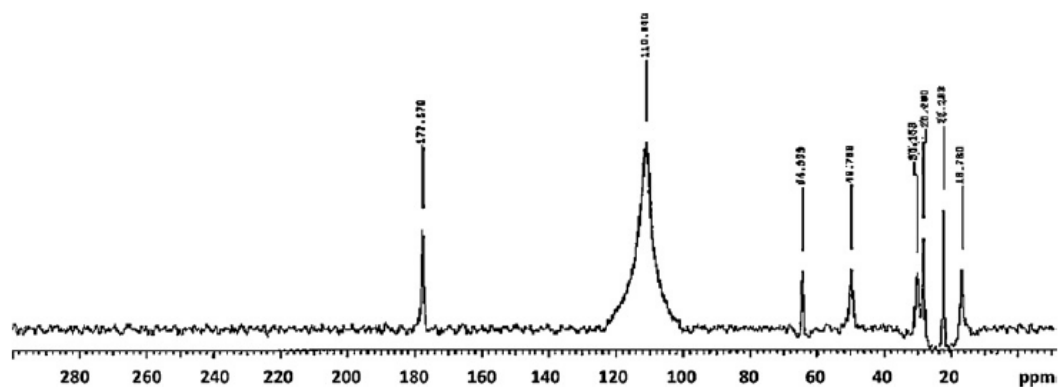


Fig. 1. ^{13}C DP-MAS NMR spectra of immobilized Cr-catalyst (LCI).

Requisite amount of catalyst (0.010 g) was added to the reaction mixture, and this was taken as the starting point of the reaction. The resulting mixture was stirred at $80 \text{ }^\circ\text{C}$ for 24 h under constant flow of the appropriate atmosphere. The reaction products were analyzed using a gas chromatograph and monitored at set time intervals by withdrawing small aliquots. Samples were filtered before analysis. The oxidation products were identified by comparison with authentic samples.

3. Results and discussion

The synthesis of the organic–inorganic hybrid materials immobilized chromium catalysts are illustrated in [Scheme 1](#). Two different synthetic routes were followed to immobilize the chromium(III) complex on the surface of modified silica gel depending on the sequence of the reaction steps. Route 1, the pregrafting (LCI), consists of Schiff base condensation between APTS and salicylaldehyde and subsequent complexation with chromium metal ion followed by immobilization to generate the silica supported chromium (III) catalyst. Route 2, the post grafting (FCC): the inorganic support material was functionalized with amino groups (APTS) followed by Schiff base condensation. The heterogenized ligand was then complexed with chromium acetate hydroxide.

The catalysts employed herein were based on salicylaldiminato chromium complex bound to silica gel surfaces via propyl silane spacer.

The synthesized ligand and supported complexes were characterized by a variety of spectroscopic techniques to confirm their structures. These include solid-state NMR, FTIR, UV–vis, elemental analyses and metal/N ratio, all of which support the structure of the proposed complex. The M/N ratio suggested a 2:1 ligand to metal stoichiometry.

Structural characterization of the synthesized catalysts via the two routes is comparable albeit with a slight difference in metal loading. The loading of the amino groups was 0.10 and 0.11 mmol g⁻¹ silica for 0.52 and 0.57% Cr, respectively.

3.1. NMR spectra

The H-NMR spectral data (1 in ppm) of silane Schiff base ligand (APTSsal) exhibits singlets at 8.34 and 13.56 ppm, which are attributed to azomethine and phenolic OH protons, respectively. A multiplet peak in the region 6.82–7.34 ppm is attributed to the aromatic protons. 2-Proton triplet peaks between 0.64–0.73 and 3.56–3.63 ppm are assigned to (Si CH₂) and (N CH₂) protons, respectively. A quintet in the region 1.75–1.87 ppm is assigned for (CH₂) of the propyl group. Protons of ethoxy groups exhibit a triplet at 1.19–1.26 ppm and quartet at 3.77–3.88 ppm.

Carbon-13 NMR of the ligand shows peaks at 9.47 (SiCH₂, propyl), 11.32 (CH₃, ethoxy), 23.74 (CH₂, propyl), 60.80 (CH₂, ethoxy), 86.21 (NCH₂, propyl), 116.62 (Ar), 118.00 (Ar), 118.54 (Ar), 130.85 (Ar), 131.64(Ar), 161.16 (COH) and 164.32 (CN) ppm.

The supported ligand on silica was characterized by C-13 solid-state NMR spectroscopy to confirm the incorporation of silane Schiff base ligand on the support. The ¹³C CP-MAS experiment of the supported complex was not successful due to the presence of paramagnetic chromium.

Fig. 1 shows the ^{13}C DP/SPE-NMR spectrum of the immobilized catalyst (LCI). The spectrum shows peaks at 16.8, 28.3 and 49.8 ppm which were attributed to the different methylene carbons of the propyl group in the linker showing the incorporation of amine functional groups. This is in agreement with the reported results on similar silane modified silica [23]. The peak at 24 ppm is assigned to the CH_3 [24] whereas, azomethine carbon could be hardly observed. The peak ~ 178 ppm is assigned to carbonyl carbon of the bridging acetate group.

The presence of peak in the high field region (114 ppm) is typical of the carbon resonances for an aromatic system. The ^{29}Si CPMAS NMR spectrum of the silica support shows three resonance peaks at chemical shifts $\delta = -111$ (Q^4), -101 (Q^3), and -92 (Q) ppm which are assigned to the silica framework [25]. Immobilization of the ligand onto the surface makes the Q^2 peak featureless, whereas the intensities of Q^3 peak decreases and concomitantly increases the Q^4 peak as shown in Fig. 2. This is due to the consumption of isolated Si-OH groups and geminal silandiols during the reaction.

The ^{29}Si NMR proves that the APTS was successfully grafted on the surface in agreement with C/N analysis. This is concluded by the absence of the ungrafted APTS resonance signal which would appear at -45 ppm and the appearance of an additional broad resonance peak at -64 ppm created by overlapping two peaks at distinct chemical shifts corresponding T^2 and T^3 [26].

3.2. UV-visible spectra:

The electronic spectra of the unsupported complex and immobilized catalyst were obtained as DR-UV or as nujol mulls (as described in the experimental section) due to their insolubility. The UV-visible spectra of these two complexes show four absorption bands at 222, 261(sh), 391 and 556 nm (Fig. 3). The first two bands are assigned to $c/ \rightarrow c/^*$ and $n \rightarrow n^*$ (which belong to an intra-ligand transition at 213 and 256 nm, respectively). The other two bands are assigned to symmetry forbidden charge transfer transitions from the metal to the anti-bonding orbital of the ligand $4A_{2g}(F) \rightarrow 4T_{1g}(F)$, which appeared as a broad band at 391 nm similar to that reported for analogue systems [27]. A very weak and broad absorption band appearing in the complex at 556 nm (highly concentrated sample was used), due to d-d transition, $4A_{2g}(F) \rightarrow 4T_{2g}(F)$ (v) [28], merged with the $n \rightarrow n^*$ spin allowed internal ligand transition band [10]. A weak shoulder appearing in the ligand spectrum at 299 nm is assigned as intramolecular hydrogen bonding, which disappeared in the spectra of the complexes.

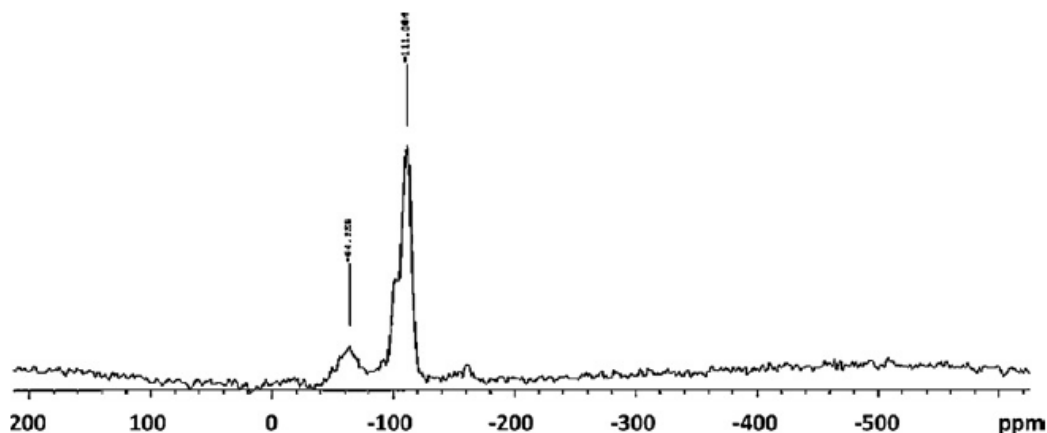


Fig. 2. ^{29}Si CP-MAS NMR spectra of immobilized Cr-catalyst (LCI).

This indicates the coordination of phenolic oxygen to the metal ion. The electronic spectra of the supported catalysts exhibit similar bands to that reported for similar systems [29], which indicate the existence of the same coordination environment around chromium(III).

3.3. Infrared spectra

FT-IR spectroscopy was used to confirm the functionalization of the support (Fig. 4). The intensities of the bands of the supported metal complex were weak due to low concentration of the metal complex.

The supported and unsupported ligand (APTSSal) exhibit a band at 1632 cm^{-1} assigned to ν (C N) of the azomethine stretching vibration band which is shifted to a lower frequency (1614 cm^{-1}) on complexation due to coordination of the azomethine nitrogen atom to the metal ion. The appearance of two to three bands in the spectra of the complex in the low frequency region (between 410 and 527 cm^{-1}) is attributed to ν (M N and M O) stretching, which indicates the coordination of the phenolic oxygen as well as the azomethine nitrogen to the metal ion [14b],[30].

The ligand (APTSSal) exhibits a band at 3058 cm^{-1} , that is assignable to ν (OH phenolic) which disappeared on complexation [31,32]. The band at 1280 cm^{-1} is assigned to the deformation vibration, ρ (O-H phenolic) in plane overlapped with the Si-O asymmetric stretching vibration band of silica.

Further absorptions in the range of 3000 , 2880 – 2980 and 1455 cm^{-1} are assigned to aromatic C H stretching, aliphatic C H stretching and deformation vibrations, respectively [33]. The Si O Si stretching and bending vibrations in the silanol Schiff base ligand which appeared at ~ 1040 and $\sim 805\text{ cm}^{-1}$ were not affected [31,34].

The supported Cr-catalyst shows a broad band at $\sim 3480\text{ cm}^{-1}$ which is assigned to O H stretching vibrations of silanol groups overlapped with the symmetric stretching vibrations of H_2O [35]. The supported catalyst shows a strong absorption at 1712 cm^{-1} due to the C O stretching vibration of the acetate group. Additionally, the catalyst shows stretching vibration peaks at 1543 and 1410 cm^{-1} , which are attributed to the asymmetric and symmetric stretching modes of the CO_2 group in the bridging acetate. The difference between the two band positions ($L_1 = 133\text{ cm}^{-1}$) is considerably less than that found for ionic acetate ($164\text{--}171\text{ cm}^{-1}$) and can be attributed to the presence of the bridging carboxylate group [36].

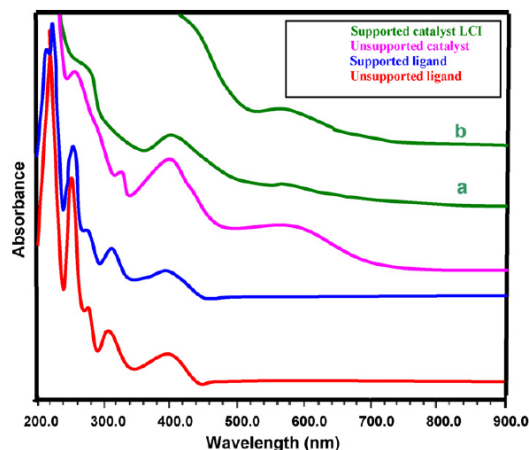


Fig. 3. Electronic spectra of the unsupported and supported ligand, unsupported and supported complex (a) diluted and (b) concentrated.

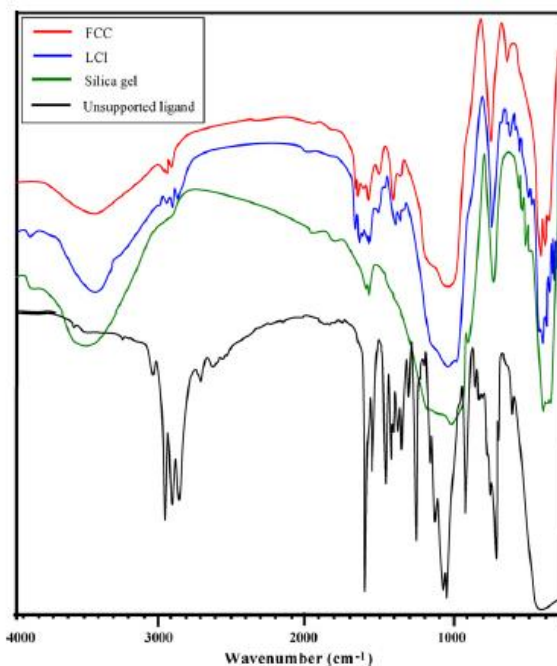


Fig. 4. FT-IR spectral pattern of the support and the supported and unsupported catalysts.

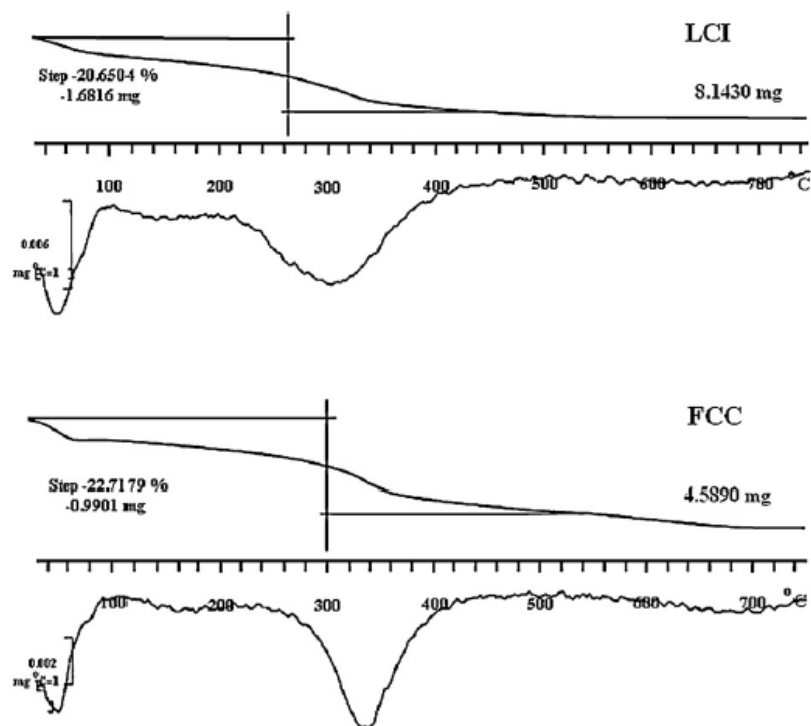


Fig. 5. TGA-DTG thermograms for supported Cr-catalysts.

A similar bridging dinuclear structure was confirmed by X-ray crystal structure analysis for copper complex related systems, which further supports the structure of our complex [37]. The proposed structure of the bridging unit is in agreement with the elemental analysis and supported by a number of previous examples of binuclear Cr(III) complexes [38] in which the Cr(III) centres are linked by one acetate and one hydroxo bridge. From the above results it may be concluded that the donor ligands which act as NO bidentate, and the bridging groups, fill the octahedral coordination about the chromium ion. Interestingly, the bridging binuclear complex was obtained on using chromium acetate hydroxide as a metal source, while mononuclear octahedral complex was obtained using chromium acetate [7]. These results confirm introduction of the bridged chromium complex onto the silica support.

3.4. Thermal analysis

TGA-DTG thermograms of supported Cr-catalysts show that the amount of the metal loading in both routes is equivalent to the % metal obtained from atomic absorption and ICP (Fig. 5) i.e. the content of combustible organic ligand and bridging groups is in stoichiometric proportion to the metal amount found by ICP. The supported complexes synthesized via route 1 and 2 (Scheme 1) exhibit similar TGA-DTG traces.

The immobilized complex shows a three-stage loss. The weight loss peaks below 120 °C with a mass loss of 4.1–4.3% is due to physically adsorbed water. The following decomposition steps consist of: (i) elimination of bridging acetate and hydroxyl

moieties at about 160–180 °C, which is expected to fall in the range of 120–300 °C [39]; (ii) decomposition of the ligand starts in the range of 300–320 °C. This step starts immediately after the previous step and ends at ca. 450 °C. Unfortunately, it is difficult to estimate loss percent in both stages separately due to overlapping of the two steps between 180 and 450 °C with an overall weight loss of 17.4% for FCC and 16.6% for LCI.

3.5 Surface area analysis

Nitrogen physisorption was used to determine the changes in the BET surface area, average pore diameter, and pore volume of the silica resulting from immobilization of the Cr-complex. The surface area and total pore volume of silica gel and the immobilized catalysts prepared via routes 1 and 2 are shown in Table 1. This information is quite important to compare the adsorption properties of silica gel and immobilized catalysts.

Nitrogen adsorption–desorption isotherms of the catalysts revealed a reversible type IV behaviour [40]. The supported Cr-catalysts synthesized via routes 1 and 2 show a decrease in the value of the surface area indicating the influence of immobilized complex on the silica gel surface. The surface areas, pore volumes and pore sizes of the catalysts decrease as a function of increasing the loading; however the increase in loading results in increased crowding of the functionalized groups in the pores. Thus, the pore size of LCI catalyst is less affected by the crowding as a result of less loading. Although the two materials are synthesized under similar conditions with equal amounts of precursor solution, metal loading in catalyst FCC is ~10% higher than LCI.

3.6 Catalytic activity study

To evaluate the catalytic behaviour of the Cr-catalysts prepared, oxidation of cyclohexene was carried out in different solvents and under various reaction conditions. Cyclohexene is a suitable test reagent for the oxidation of alkenes due to the low stability of the resultant epoxide as well as the range of products formed (Equation 1).

Table 1
Textural properties of the support and the catalysts.

Support/catalyst	BET surface area (m ² /g)	Pore volume (cm ³ /g)	Pore size* (Å)	%wt M content
Silica gel (Davisil 710)	347.5	0.77	88.30	–
Cr-catalyst LCI (Route 1)	235.0	0.52	87.79	0.52
Cr-catalyst FCC (Route 2)	221.6	0.49	83.13	0.57

* Pore size distributions were calculated from the desorption branch by using BJH method.

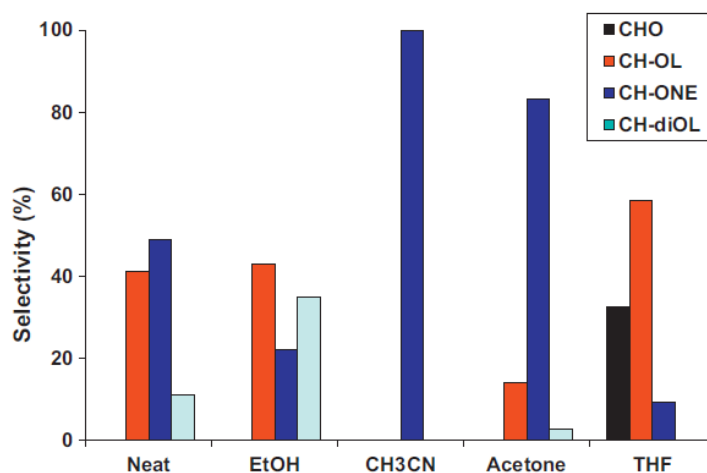
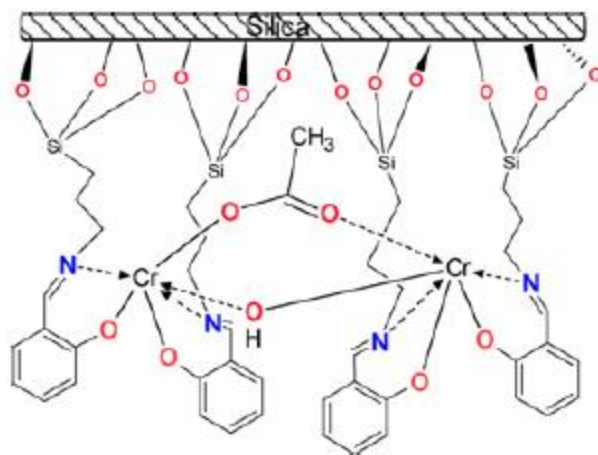


Fig. 6. Selectivity (%) to various oxidation products under O_2 atmosphere using Cr-supported catalyst (LCI) at 6 h reaction time under the optimized conditions: cyclohexene (0.025 mol), catalyst (10 mg), cyclohexene:oxidant (1:1 molar ratio), solvent (THF; 2 mL) and temperature ($80^\circ C$).

3.7. Oxidation under aerobic conditions

The catalytic activity of the silica supported Cr-complex (LCI; route 1) as a representative cyclohexene catalyst was initially studied in an aerobic atmosphere using a wide range of solvents and H_2O_2 as an oxidant (Table 2). It was found that the % conversion was dependent on the polarity of the solvent. Using polar solvents such as THF, MeCN, EtOH and acetone, the % cyclohexene conversion varied between 8–72% over 6 h reaction period. Extending the reaction time to 24 h increased the conversion to 38–80% depending on the solvent used. In non-polar solvents such as benzene and 1,2-dichloroethane, cyclohexene was oxidized to a considerably lower extent. This may be due to a non-homogeneous reaction mixture (two-phase solvent system). The same effect was found when the oxidation reaction was carried out in bulk (solventless). The reaction time also has an impact on the product selectivity. In general, under these conditions cyclohexene oxidation proceeds with higher selectivity for 2-cyclohexen-1-ol (21–37%) and 2-cyclohexen-1-one (14–46%).

3.8. Oxidation in inert atmosphere

To ascertain the extent to which molecular oxygen in air may play a role in the oxidation, similar oxidation reactions were carried out under anaerobic conditions (under N₂), to gain further insight into the role of oxygen on the % conversion and selectivity of cyclohexene oxidation.

Table 2 shows that the catalyst was most inactive or much less active (~1–37% conversion, 6 h). On the other hand, the effect of solvent under an anaerobic atmosphere has a similar pattern compared to that under an aerobic atmosphere with almost similar products selectivity. There is no significant increase in conversion after 24 h (3–44%). From the results above it can be concluded that oxygen plays a major role in the oxidation process as a co-oxidant.

3.9. Oxidation in oxygen atmosphere

To further confirm the effect of oxygen and to prove its role as a co-oxidant, the reaction was investigated under an oxygen atmosphere using four selected solvents (Table 2). A significant increase in the cyclohexene conversion was observed reaching 94% in THF after 6 h and quantitative after 24 h. Selectivity in the formation of various cyclohexene oxidation products under an oxygen atmosphere in different solvents is shown in Fig. 6. Cyclohexene oxide was only detected when the reaction was conducted in THF solvent along with other expected products. In neat (solvent-free) solution and ethanol, only three products viz. 2-cyclohexene-1-ol, cyclohexene-1-one and 1,2-cyclohexandiol were detected. Using acetonitrile, 100% selectivity towards 2-cyclohexen-1-one was obtained. It is noteworthy to mention that the product selectivity was dependent upon the type of solvent used [41–43]. Furthermore, when these catalysts were tested under an oxygen atmosphere in the absence of H₂O₂, these results verified that the oxygen plays an important role in the oxidation process as a co-oxidant.

Table 2
Cyclohexene conversion (%) under various atmospheres at two different time intervals in different solvents using Cr-supported catalyst (LCI).

Atmosphere	Time (h)	Cyclohexene conversion (%) / Solvent						
		Neat	EtOH	MeCN	Benzene	DCE	Acetone	THF
Air	6	0	8.0	40.2	1.2	0.6	62.7	72.1
	24	29.1	38.4	55.5	5.4	21.5	71.2	80.1
Nitrogen	6	0	14.0	0	0	3.6	36.7	19.5
	24	5.8	15.1	31.3	2.4	7.7	43.8	23.4
Oxygen	6	52.2	69.0	61.6	6.3	16.7	66.8	93.6
	24	81.5	85.2	89.4	29.2	48.9	69.3	>99.0

Reaction conditions: cyclohexene (0.025 mol); H₂O₂ (0.025 mol); catalyst (10 mg); temp. 80 °C; solvent (2 mL).

Table 3
Effect of H₂O₂:cyclohexene molar ratio on cyclohexene conversion (%) and %H₂O₂ efficiency.

Reaction time(h)	H ₂ O ₂ :cyclohexene molar ratio					
	0.5:1		1:1		2:1	
	% Conversion	% H ₂ O ₂ efficiency	% Conversion	% H ₂ O ₂ efficiency	% Conversion	% H ₂ O ₂ efficiency
1	28.4	44.6	40.7	32.7	62.1	24.1
2	33.7	52.9	48.2	37.5	81.1	31.2
6	76.8	100.0	93.6	72.4	100.0	40.4

Reaction conditions: cyclohexene (0.025 mol); catalyst (10 mg); temperature 80° C, solvent THF (2 mL). %H₂O₂ efficiency = (moles of H₂O₂ utilized in products formation/moles of H₂O₂ added) × 100.

3.10. Optimization of other reaction conditions

To optimize the reaction conditions under an oxygen atmosphere for cyclohexene oxidation, other parameters such as temperature, time, substrate:oxidant molar ratio, volume of solvent, catalyst weight, additive, and oxidant were studied in detail.

3.11. Effect of amount of catalyst

Different amounts of catalyst were employed to investigate the corresponding variation on the oxidation results as shown in Fig. 7. The % cyclohexene conversion increased from 80 to 94% on increasing the catalyst weight from 5 to 10 mg. Even 5 mg catalyst was efficient to catalyze the oxidation reaction. These results confirm that Cr-supported catalyst is highly active for oxidation of cyclohexene. As the catalyst amount increased the % H₂O₂ decomposition will increase which in turn decrease the oxidation process i.e. lower conversion.

3.12. Effect of volume of solvent

The volume of solvent has a significant effect on the % conversion when using THF. Increasing the volume of solvent from 2 to 5 mL causes the % conversion to decrease from 94 to 42% at 6 h and to 61% after 24 h. Further increases in the volume of solvent results in dramatic decreases in conversion as shown in Fig. 8. The reduced rate of reaction observed upon increasing the volume of solvent may be due, in part, to the decrease in the bulk density of the catalyst particles in the reaction media. The effect of the solvent's volume in agreement with the effect of amount of catalyst (vide infra).

3.13. Effect of cyclohexene: oxidant molar ratio

The influence of H₂O₂ to cyclohexene molar ratio on the oxidation of cyclohexene under an oxygen atmosphere as a function of time is presented in Table 3. Three different H₂O₂:cyclohexene molar ratios (0.5:1, 1:1 and 2:1) were used in this study while keeping all the other parameters fixed. It is clearly shown that 2:1 molar ratio gave the maximum percentage conversion (100%) with 40% H₂O₂ efficiency after 6 h. On the other hand, the 1:1 molar ratio of the oxidant:cyclohexene gave 94% overall cyclohexene conversion with 72% H₂O₂ efficiency. Reducing the molar ratio to 0.5:1, i.e. H₂O₂ in half molar amount of cyclohexene, the overall percentage conversion was lowered to ca. 77% with 100% H₂O₂ efficiency (Table 3).

These results suggest that 1:1 molar ratio is the minimum requirement for the effective oxidation of cyclohexene along with better percentage H₂O₂ efficiency. This clearly suggests that a large concentration of oxidant is not an essential condition to maximize cyclohexene transformation. Obviously, an increase in H₂O₂ concentration enhanced the decomposition of H₂O₂ to form oxygen and hence the side reactions, including allylic oxidation [43,44]. After 8 h of using 1:1 molar ratio, a maximum conversion was achieved ~100%, whereas on using 0.5:1 molar ratio the maximum conversion of 91% was levelled off after 12 h reaction time.

3.14. Effect of other oxidant and additive

The oxidation of cyclohexene was carried out using an oxidant other than H₂O₂, namely 70% aqueous *tert*-butylhydroperoxide. This oxidant was unable to oxidize cyclohexene under the optimized reaction conditions. The overall conversion obtained was less than 4%. It seems that this oxidant failed to generate active oxidant species and also had solubility problems associated with the reactant *vis-a-vis* the oxidant.

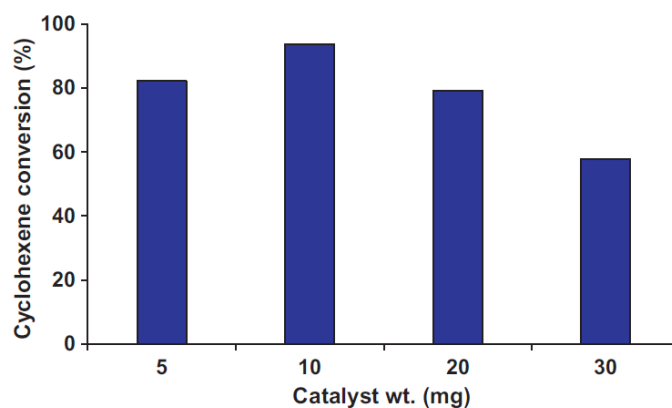


Fig. 7. Effect of amount of catalyst on cyclohexene conversion under O₂ atmosphere using Cr-supported catalyst (LCI) at 6 h reaction time under the optimized conditions: cyclohexene (0.025 mol), cyclohexene:oxidant (1:1 molar ratio), solvent (THF; 2 mL) and temperature (80 °C).

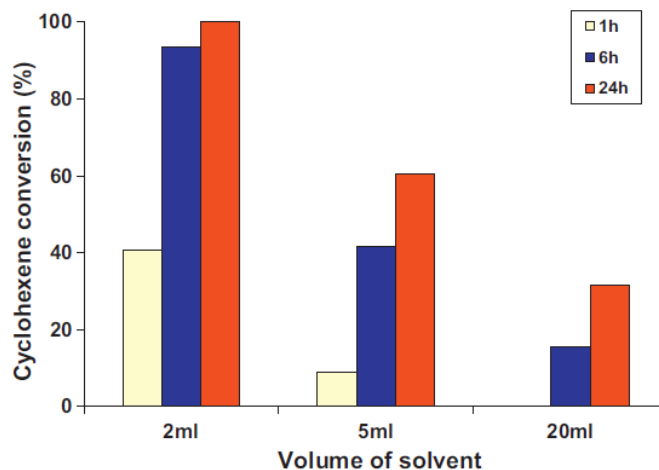


Fig. 8. Effect of volume of solvent on % cyclohexene conversion under O₂ atmosphere using Cr-supported catalyst (LCI) at 6 h reaction time under optimized conditions: cyclohexene (0.025 mol), catalyst (10 mg), cyclohexene:oxidant (1:1 molar ratio), solvent (THF) and temperature (80 °C).

Table 4

Comparison study between the as-prepared catalysts and their metal source.

Reaction time (h)	(L.C.I.) route 1		(F.C.C.) route 2		Cr-acetate hydroxide	
	Conv. (%)	TOF (h ⁻¹)	Conv. (%)	TOF (h ⁻¹)	Conv. (%)	TOF (h ⁻¹)
1	40.7	10174	63.0	14367	82.2	413
2	48.2	6025	71.3	8130	87.4	209
6	93.6	3900	>99.0	3763	>99.0	83

Reaction conditions: cyclohexene (0.025 mol); H₂O₂ (0.025 mol); catalyst (10 mg); temperature 80 °C, THF (2 mL). Turn over frequency (TOF).

Hence, hydrogen peroxide is a preferred oxidant as it is environmentally friendly and produces only water as by-product and shows good selectivity.

Studies have shown that ascorbic acid as an additive may play a role in the epoxidation of alkenes using H₂O₂ as oxidant [45]. In this study, ascorbic acid in the presence of H₂O₂ was also used. No marked effect was observed using ascorbic acid on either activity or selectivity.

3.15. Comparison study for catalysts' performance

After optimizing the reaction conditions (cyclohexene (0.025 mol), catalyst (10 mg), 1:1 cyclohexene:oxidant molar ratio, THF (2 mL) and temperature (80 °C) under an oxygen atmosphere), a comparison study between Cr-based catalysts (LCI and FCC) and chromium acetate hydroxide was performed for the oxidation of cyclohexene. From Table 4, it is evident that the Cr-based catalyst (LCI) shows lower performance (41% conversion) in comparison with FCC catalyst 63% after 1 h reaction time.

However the LCI catalyst performs much better after 6 h and catalyzes the oxidation of cyclohexene with a maximum of 94% conversion comparable to FCC and the homogenous catalysts.

For a meaningful comparison of the relative performances of the catalysts, turn over frequency values (TOF) should be used. TOF values have been calculated on the basis of the total chromium ions present in the solid catalyst. The immobilized complexes exhibit much higher TOF values by several orders of magnitude than the metal source used in this work (>45 times). In fact, significant enhancement in the intrinsic activity compared to metal source is a strong indication that it is the catalytic behaviour of the immobilized metal complexes which is responsible for the observed enhancement. As no leaching was detected the catalytic activity may be described to the immobilized complexes.

On comparing the catalytic data obtained herein for the oxidation of cyclohexene using H₂O₂ with the reported data (% conversion, catalyst wt., reaction time, oxidant); Cr-MCM-41 (52%, 20 mg, 24 h, O₂) [15], Cr-MCM-48 (67%, 50 mg, 12 h, TBHP) [42] as well as other chromium-based catalyst (~70%, 600 mg, 6 h, O₂) [46], our catalysts show excellent conversion at a shorter reaction time and required less amount of catalyst. While our catalysts show very low activity under dioxygen atmosphere or using TBHP as an oxidant.

In terms of product selectivities, 2-cyclohexen-1-ol was the only product detected after the first hour of reaction and then decreased with time to level off after 3 h. Meanwhile, selectivity towards 2-cyclohexen-1-one increased markedly to a maximum after 3 h (~80%). Cyclohexene oxide starts to form after 1 h and reaches the maximum of ~32% at 2 h and then demolish within the next hour. 1,2-Cyclohexandiol starts to form after ~2 h and its concentration increased with increasing reaction time. After 6 h the selectivity for the products levels off. Cyclohexene oxide was obtained only in THF at moderate-low percentage, and decreased with time, possibly due to instability of the epoxide, which undergoes ring-opening reaction (Fig. 9). Under similar conditions and extending the reaction time to 24 h, the conversion was increased slightly with a slight change in the selectivity of the products.

The insignificant difference in activity between the two catalysts (FCC and LCI) may be due to the minor difference in % metal content. Both catalysts catalyze olefin oxidation efficiently with very high selectivity for partially oxidized products (>90%).

3.7 Reusability

In order to examine the reusability of the catalyst, it was separated from the reaction mixture by filtration, thoroughly washed with acetonitrile and finally dried at 120 °C and reused three times under similar conditions. The recycled catalyst was found to exhibit almost the same conversion, 94.2, 93.7 and 92.4% after the first, second and third recycling, respectively. To test for the absence of metal leaching, the catalyst was separated from the reaction mixture by filtration at the reaction temperature after 2 h and the reaction mixture was allowed to react further. No additional

conversion of cyclohexene was observed after removal of the catalyst. The ICP analysis of the reaction mixture confirms that no chromium metal was detected. This positively suggests that metal leaching does not occur and is indicative of chemical bonding between the metal and the support of the catalyst. However, the selectivity towards the products after 6 h remains unaffected. Comparable IR spectra between fresh and used catalysts indicates no change in the functionalities and that catalytic behaviour should still be possible.

3.8 3D modelling optimized geometry

In order to estimate the geometry of the complex 3-dimensional molecular modelling for $(\mu\text{-acetato})(\mu\text{-hydroxo})$ -bridged dichromium(III) complex using HyperChem Version 6.01 was performed.

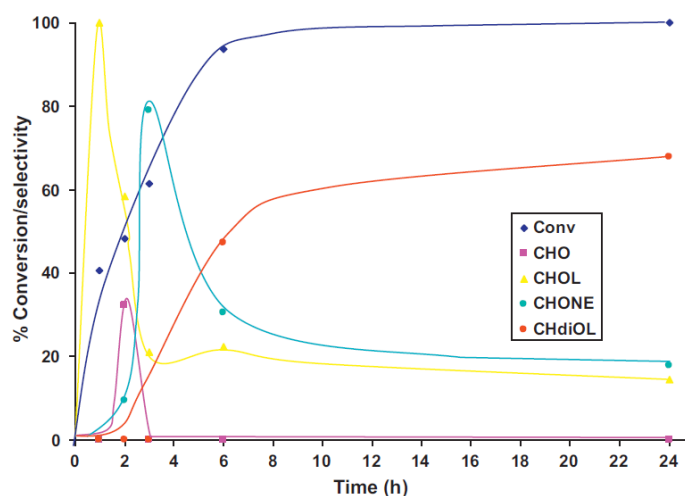


Fig. 9. Effect of reaction time on % cyclohexene conversion and selectivity under O_2 atmosphere using Cr-supported catalyst (LCI) under optimized conditions: cyclohexene (0.025 mol), catalyst (10 mg), cyclohexene:oxidant (1:1 molar ratio), solvent (THF; 2 mL) and temperature ($80^\circ C$).

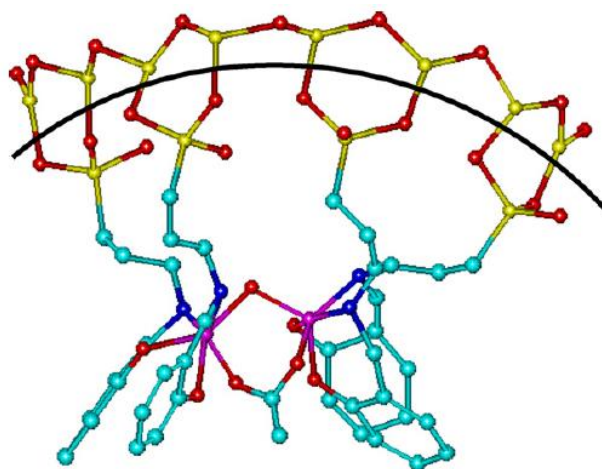


Fig. 10. Structural model of chromium complex immobilized on silica gel surface; hydrogen atoms have been omitted for clarity. The black curve represents the silica surface.

To calculate the bond lengths and dihedral angles (torsion angle) between the chromium metal centres and the phenyl rings of the ligands, Parametric Method (PM3) was used performing the semi-empirical Self-Consistent Field (SCF) theory for the geometric optimization. The structural model of the complex is shown in Fig. 10. It is clear the structure of the complex consists of binuclear metal in which the two Cr(III) centres are linked by one acetato and one hydroxo group, with nitrogen and oxygen atoms from the salicylidiminto ligands completing a distorted octahedral geometry around each metal centre.

Two [Cr(L2)] units are bridged by one hydroxo and one acetato ligand to give a chromium to chromium separation of 3.30138 \AA . The Cr(1)–O(OH)–Cr(2) angle in the bridge is 118.24° , while the O(OH)–Cr(1)–O(OAc) and O(OH)–Cr(2)–O(OAc) angles are 100.60 and 97.67° , respectively. The Cr–O bond lengths to the carboxylate oxygens are shorter than those to the hydroxide bridge. The Cr–O bond lengths for the acetate are (Cr(2)–O(OAc) 1.9082 \AA and Cr(1)–O(OAc) 1.9002 \AA) and for the hydroxo bridge, the Cr(1)–O(OH) and Cr(2)–O(OH) are 1.9189 and 1.9151 \AA , respectively. These values are in agreement with those found for the previously reported bridged-(acetate)(hydroxo)-Cr(III) complexes [38,47]. The acetate bridging group causes considerable lengthening of the Cr–Cr distance. The need to accommodate the acetate bridging group results in a wider Cr(1)–O(OH)–Cr(2) angle of 118.24

4. Conclusion

Active catalysts supported on a chemically modified silica gel with 3-aminopropyltriethoxysilane via two synthetic routes were synthesized and characterized. The elemental and spectroscopic analyses support the assigned structure of the complex and confirmed that the synthesized catalysts were identical.

Catalytic activity of supported Cr catalysts (LCI and FCC) under an oxygen atmosphere for cyclohexene oxidation with H_2O_2 was found to be as productive as for the homogeneous analogue (chromium acetate hydroxide). However LCI and FCC catalysts were less active under a nitrogen atmosphere. Oxidation of cyclohexene using H_2O_2 in air, nitrogen and oxygen atmospheres in the presence of LIC and FCC catalysts proceeds mainly at the allylic and olefin bond. Efficiency of LCI and FCC catalysts for oxidation of cyclohexene in different solvents decreases in the order: THF > acetone > acetonitrile > ethanol > solventless > 1,2-dichloromethane > benzene.

Factors that influence the oxidation were also rigorously investigated and the optimum reaction conditions were: cyclohexene (0.025 mol), catalyst (10 mg), cyclohexene:oxidant (1:1 molar ratio), solvent (THF; 2 mL) and temperature (80°C) under an oxygen atmosphere.

Cyclohexene oxide was obtained only in THF (32%) after 2 h and decreased with time due to epoxide ring-opening.

Furthermore, the silica-supported chromium could be recovered and recycled by a simple filtration of the reaction mixture and used for 3 consecutive trials without loss of activity. Recycled catalysts exhibited similar activity which suggests the true heterogeneous nature of the catalyst.

Acknowledgments

The authors are grateful to the University of the Western Cape for their financial support.

References

[1]

(a) C. Baleizao, B. Gigante, H. Garcia, A. Corma, *Journal of Catalysis* 215 (2003) 199–207;

(b) C. Li, *Catalysis Reviews -Science Engineering* 46 (2004) 419–492;

(c) J.M. Thomas, *Angewandte Chemie International Edition* 38 (1999) 3589–3628.

[2] J.H. Clark, *Catalysis of Organic Reactions using Supported Inorganic Reagents*, VCH, New York, 1994.

[3]

(a) P. McMorn, G.J. Hutchings, *Chemical Society Review* 33 (2004) 108–122;

(b) C.E. Song, S.-G. Lee, *Chemical Review* 102 (2002) 3495–3524;

(c) Q.-H. Xia, H.-Q. Ge, C.-P. Ze, Z.-M. Liu, K.-X. Su, *Chemical Review* 105 (2005) 1603–1662;

(d) Q.-H. Fan, Y.-M. Li, A.S.C. Chan, *Chemical Review* 102 (2002) 3385–3466;

(e) D. Brunel, N. Belloq, P. Sutra, A. Cauvel, M. Lasperas, P. Moreau, F. Di Renzo, A. Galarneau, F. Fajula, *Coordination Chemistry Reviews* 178 (1998) 1085–1108;

(f) R.M. Martín-Aranda, J. Cejka, *Topics in Catalysis* 53 (2010) 141–153;

(g) S.L. Jain, B.S. Rana, B. Singh, A.K. Sinha, A. Bhaumik, M. Nandi, B. Sain, *Green Chemistry* 12 (2010) 374–377.

[4]

(a) C. Capel-Sanchez, J.M. Campos-Martin, J.L.G. Fierro, *Catalysis Today* 158 (2010) 103–108;

(b) S.M. Bruno, J.A. Fernandes, L.S. Martins, I.S. Goncalves, M. Pillinger, P. Ribeiro-Claro, J. Rocha, A.A. Valente, *Catalysis Today* 114 (2006) 263–271;

(c) P.M. Price, J.H. Clark, D.J. Macquarrie, *Journal of Chemical Society, Dalton Transaction* (2000) 101–110.

[5] L. Alaerts, J. Wahlen, P.A. Jacobs, D.E. De Vos, *Chemical Communication* (2008) 1727–1737.

[6]

(a) Y. Rohlfig, D. Wöhrle, J. Rathousky, A. Zukal, M. Wark, *Studies in Surface Science and Catalysis* 142 (2002) 1067–1074;

(b) V. Antochshuk, O. Olkhovyk, M. Jaroniec, I.-S. Park, R. Ryoo, *Langmuir* 19 (2003) 3031–3034;

(c) E.J. Acosta, C.S. Carr, E.E. Simanek, D.F. Shantz, *Advanced Materials* 16 (2004) 985–989;

(d) I. Slowing, B.G. Trewyn, V.S.-Y. Lin, *Journal of the American Chemical Society* 128 (2006) 14792–14793.

[7]

(a) E.P. Plueddemann, *Silane Coupling Agents*, 2nd ed., Plenum, New York, 1991;

(b) K.L. Mittal, *Silanes and Other Coupling Agents*, vol. 2, VSP, Utrecht, The Netherlands, 2000.

- [8] A.M. Liu, K. Hidajat, S. Kawi, D.Y. Zhao, *Chemical Communication* (2000) 1145–1146.
- [9] J.F. Díaz, K.J. Balkus, *Journal of Molecular Catalysis B: Enzymatic* 2 (1996) 115–126.
- [10] F. Balas, M. Manzano, P. Horcajada, M. Vallet-Regi, *Journal of the American Chemical Society* 128 (2006) 8116–8117.
- [11]
- (a) K.K. Sharma, T. Asefa, *Angewandte Chemie International Edition* 46 (2007) 2879–2882;
- (b) K.K. Sharma, A. Anan, R.P. Buckley, W. Ouellette, T. Asefa, *Journal of the American Chemical Society* 130 (2008) 218–228;
- (c) X. Wang, K.S.K. Lin, J.C.C. Chan, S. Cheng, *Journal of Physical Chemistry B* 109 (2005) 1763–1769;
- (d) D.J. Macquarrie, D.B. Jackson, *Chemical Communication* (1997) 1781–1782;
- (e) A. Cauvel, G. Renard, D. Brunel, *Journal of Organic Chemistry* 62 (1997) 749–751;
- (f) S.-C. Sujandi, D.-S. Han, M.-J. Han, S.-E. Jin, Park, *Journal of Catalysis* 243 (2006) 410–419;
- (g) H. Balcar, J. Cejka, J. Sedlacek, J. Svoboda, J. Zednik, Z. Bastl, V. Bosacek, J. Vohlidal, *Journal of Molecular Catalysis A* 203 (2003) 287–298.
- [12]
- (a) F. Fache, E. Schulz, M.L. Tommasino, M. Lemaire, *Chemical Review* 100 (2000) 2159–2232;
- (b) E.N. Jacobsen, in: I. Ojima (Ed.), *Catalytic Asymmetric Synthesis*; VCH, New York, 1995;
- (c) E.N. Jacobsen, in: E.W. Abel, F.G.A. Stone, G. Wilkinson (Eds.), *Comprehensive Organometallic Chemistry II*; vol. 12, Pergamon, New York, 1995;
- (h) R.A. Sheldon, in: R. Ugo (Ed.), *Aspects of homogeneous catalysis*, vol. 4, D. Reidel Dordrecht, 1981;
- (i) E.M. McGarrigle, D.G. Gilheany, *Chemical Review* 105 (2005) 1563–1602;
- (j) P. Jin, Z. Zhao, Z. Dai, D. Wei, M. Tang, X. Wang, *Catalysis Today* 175 (2011) 619–624.
- [13]
- (a) P.E. Aranha, M.P. dos Santos, S. Romera, E.R. Dockal, *Polyhedron* 26 (2007) 1373–1382;
- (k) E.G. Samsel, K. Srinivasan, J.K. Kochi, *Journal of the American Chemical Society* 107 (1985) 7606–7617;
- (l) E.M. McGarrigle, D.M. Murphy, D.G. Gilheany, *Tetrahedron: Asymmetry* 15 (2004) 1343–1354;
- (m) N.J. Kerrigan, H. Muller-Bunz, D.G. Gilheany, *Journal of Molecular Catalysis A* 227 (2005) 163–172.
- [14]
- (a) W.G. Dauben, M. Lorber, D.S. Fullerton, *Journal of Organic Chemistry* 34 (1969) 3587–3592;

- (b) J. Muzart, *Chemical Review* 92 (1992) 113–140.
- [15] S.E. Dapurkar, H. Kawanami, K. Komura, T. Yokoyama, Y. Ikushima, *Applied Catalysis A: General* 346 (2008) 112–116.
- [16] Y. Shiraishi, Y. Teshima, T. Hirai, *Journal of Physical Chemistry B* 110 (2006) 6257–6263.
- [17] S.K. Mohapatra, P. Selvam, *Journal of Catalysis* 249 (2007) 394–396.
- [18]
- (a) B.M.L. Dooos, P.A. Jacobs, *Applied Catalysis A: General* 282 (2005) 181–188.
- [19] I.C. Chisem, J. Rafelt, J. Chisem, J.H. Clark, D. Macquarrie, M.T. Shieh, R. Jachuck, C. Ramshaw, K. Scott, *Chemical Communication* (1998), 1949–1050;
- (b) X.-G. Zhou, X.-Q. Yu, J.-S. Huang, C.-M. Che, S.-G. Li, L.-S. Li, *Chemical Communication* (1999) 1789–1790.
- [20] R.A. Sheldon, J.K. Kochi, *Metal-Catalyzed Oxidations of Organic Compounds*, Academic Press, New York, 1981.
- [21]
- (a) T.L. Siddall, N. Miyaoura, J.C. Huffman, J.K. Kochi, *Journal of Chemical Society, Chemical Communication* (1983) 1185–1186;
- (b) P.A. Ganeshpure, S. Satish, *Journal of Chemical Society, Chemical Communication* (1988) 981–982;
- (c) W. Adam, M. Herold, C.L. Hill, C.R. Saha-Moller, *European Journal of Organic Chemistry* (2002) 941–946;
- (d) K.M. Ryan, C. Bousquet, D.G. Gilheany, *Tetrahedron Letters* 40 (1999) 3613–3616;
- (e) A.M. Daly, M.F. Renehan, D.G. Gilheany, *Organic Letters* 3 (2001) 663–666;
- (f) C.P. O'Mahony, E.M. McGarrigle, M.F. Renehan, K.M. Ryan, N.J. Kerrigan, C. Bousquet, D.G. Gilheany, *Organic Letters* 3 (2001) 3435–3438;
- (g) M.D. Angelino, P.E. Laibinis, *Journal of Polymer Science A: Polymer Chemistry* 37 (1999) 3888–3898;
- (h) K.B. Hansen, J.L. Leighton, E.N. Jacobsen, *Journal of the American Chemical Society* 118 (1996) 10924–10925;
- (i) A. Heckel, D. Seebach, *Helvetica Chimica Acta* 85 (2002) 913–926;
- (j) B.M.L. Dooos, P.A. Jacobs, *Tetrahedron Letters* 44 (2003) 8815–8817;
- (k) B.M.L. Dooos, W.A. Geurts, P.A. Jacobs, *Catalysis Letters* 97 (2004) 125–129;
- (l) C. Baleizao, B. Gigante, M.J. Sabater, H. Garcia, A. Corma, *Applied Catalysis A* 228 (2002) 279–288.
- [22] S. Jana, B. Dutta, R. Bera, S. Koner, *Langmuir* 23 (2007) 2492–2496.
- [23]
- (a) G.S. Caravajal, D.E. Leyden, G.R. Quinting, G.E. Maciel, *Analytical Chemistry* 60 (1988) 1776–1786;
- (b) J.J. Yang, I.M. El-Nahhal, I.-S. Chuang, G.E. Maciel, *Journal of Non-Crystalline Solids* 209 (1997) 19–39.
- [24]
- (a) J. Bliemel, *Journal of the American Chemical Society* 117 (1995) 2112–2113;

(b) K.D. Behringer, J. Bliimel, *Journal of Liquid Chromatography and Related Technologies* 19 (1996) 2753–2765.

[25]

(a) B.-H. Ye, X.-Y. Li, I.D. Williams, X.-M. Chen, *Inorganic Chemistry* 41 (2002) 6426–6431;

(b) K.D. Behringer, J. Blmel, *Inorganic Chemistry* 35 (1996) 1814–1819;

(c) M.-C.B. Salon, M. Bardet, M.N. Belgacem, *Silicon Chemistry* 3 (2008) 335–350.

[26]

(a) X.S. Zhao, G.Q. Lu, A.K. Whittaker, G.J. Millar, *Journal of Physical Chemistry B* 101 (1997) 6525–6531;

(b) S. Zhao, J. Zhao, L.-L. Lou, S. Liu, *Microporous and Mesoporous Materials* 137 (2011) 36–42;

(c) Z. Zhang, A.E. Berns, S. Willbold, J. Buitenhuis, *Journal of Colloid and Interface Science* 310 (2007) 446–455;

(d) C. Zanzottera, A. Vicente, E. Celasco, C. Fernandez, E. Garrone, B. Bonelli, *Journal of Physical Chemistry C* 116 (2012) 7499–7506.

[27]

(a) L. Spiccia, G.D. Fallon, A.M. Markiewicz, K.S. Murray, H. Riesen, *Inorganic Chemistry* 31 (1992) 1066–1072;

(b) M.R. Maurya, S.J.J. Titinchi, S. Chand, I.M. Mishra, *Journal of Molecular Catalysis A: Chemistry* 180 (2002) 201–209;

(c) M.R. Maurya, S.J.J. Titinchi, S. Chand, *Journal of Molecular Catalysis A: Chemistry* 193 (2003) 165–176;

(d) M.R. Maurya, S.J.J. Titinchi, S. Chand, *Journal of Molecular Catalysis A: Chemistry* 214 (2004) 257–264.

[28] F.A. Cotton, G. Wilkinson, *Advanced Inorganic Chemistry*, 5th ed., Wiley, New York, 1988.

[29]

(a) R.T. Ruck, E.N. Jacobsen, *Angewandte Chemie International Edition* 42 (2003) 4771–4774;

(b) P. Brandt, P.-O. Norrby, A.M. Daly, D.G. Gilheany, *Chemical European Journal* 8 (2002) 4299–4307.

[30] K. Nakamoto, *Infrared Spectra of Inorganic and Coordination Compounds*, Wiley, New York, 1963.

[31] E.F. Murphy, D. Ferri, A. Baiker, S.V. Doorslaer, A. Schweiger, *Inorganic Chemistry* 42 (2003) 2559–2571.

[32] K.S. Abou-El-Sherbini, I.M.M. Kenawy, M.A. Hamed, R.M. Issa, R. Elmorsi, *Talanta* 58 (2002) 289–300.

[33] N.B. Colthup, in: L.H. Daly, S.E. Wiberlwy (Eds.), *An Introduction to Infrared and Raman Spectroscopy*, Academic Press, San Diego, 1990.

[34] F. Hamelmann, U. Heinzmann, A. Szekeres, N. Kirov, T. Nikolova, *Journal of Optoelectronics and Advanced Materials* 7 (2005) 389–392.

[35]

- (a) F.H. Van Cauwelaert, P.A. Jacobs, J.B. Uytterhoeven, *Journal of Physical Chemistry* 76 (1972) 1434–1439;
- (b) K.S. Smirnov, *Vibrational Spectroscopy* 4 (1993) 255–259.
- [36] G.B. Deacon, R.J. Phillips, *Coordination Chemistry Review* 33 (1980) 227–250.
- [37] J.L. van Wyk, S. Mapolie, A. Lennartson, M. Hakansson, S. Jagner, *Z. Naturforsch B: Chemical Science* 62 (2007) 331–338.
- [38]
- (a) G. Novitchi, V. Ciornea, S. Shova, A. Gulea, J.-P. Costes, A.K. Powell, *European Journal of Inorganic Chemistry* (2008) 1778–1783;
- (b) S.J. Brudenell, S.J. Crimp, J.K.E. Higgs, B. Moubaraki, K.S. Murray, L. Spiccia, *Inorganica Chimica Acta* 247 (1996) 35–41;
- (c) B.G. Gafford, R.E. Marsh, W.P. Schaefer, J.H. Zhang, C.J. O'Connor, R.A. Holwerda, *Inorganic Chemistry* 29 (1990) 4652–4657.
- [39] D. Zhao, J. Feng, Q. Huo, N. Melosh, G.H. Fredrickson, B.F. Chmelka, G.D. Stucky, *Science* 279 (1998) 548–552.
- [40] S.J. Gregg, K.S.W. Sing, *Adsorption, Surface Area and Porosity*, 2nd ed., Academic Press, San Diego, 1982.
- [41] T.K. Das, K. Chaudhari, E. Nandan, A.J. Chandwadkar, A. Sudalai, T. Ravindranathan, S. Sivasanker, *Tetrahedron Letters* 38 (1997) 3631–3634.
- [42] A. Sakthivel, S.E. Dapurkar, P. Selvam, *Applied Catalysis A: General* 246 (2003) 283–293.
- [43] J.M. Fraile, J.I. García, J.A. Mayoral, E. Vispe, *Applied Catalysis A: General* 245 (2003) 363–376.
- [44]
- (a) Y. Wang, Q. Zhang, T. Shishido, K. Takehira, *Journal of Catalysis* 209 (2002) 186–196;
- (b) S.E. Dapurkar, A. Sakthivel, P. Selvam, *New Journal of Chemistry* 27 (2003) 1184–1190.
- [45]
- (a) W. Zhang, A. Basak, Y. Kosugi, Y. Hoshino, H. Yamamoto, *Angewandte Chemie International Edition* 44 (2005) 4389–4391;
- (b) J.-E. Backvall, *Modern Oxidation methods*, 2nd ed., Wiley-VCH, Weinheim, 2011.
- [46] I.C. Chisem, J.S. Rafelt, J.H. Clark, *Chemical Communication* (1997) 2203–2204. [47] (a) H. Weihe, H.U. Gdel, *Journal of the American Chemical Society* 120 (1998) 2870–2879; J. Hodgson, S. Kallesoe, S. Larsen, E. Pedersen, *Inorganic Chemistry* 22 (1983) 637–642.